Diverse two-cysteine photocycles in phytochromes and cyanobacteriochromes

Nathan C. Rockwell, Shelley S. Martin, Kateryna Feoktistova, and J. Clark Lagarias[1]

Department of Molecular and Cell Biology, University of California, Davis, CA 95616

Contributed by J. Clark Lagarias, May 22, 2011 (sent for review March 21, 2011)

Phytochromes are well-known as photoactive red- and near IR-absorbing chromoproteins with cysteine-linked linear tetrapyrrole (bilin) prosthetic groups. Phytochrome photoswitching regulates adaptive responses to light in both photosynthetic and nonphotosynthetic organisms. Exclusively found in cyanobacteria, the related cyanobacteriochrome (CBCR) sensors extend the photosensory range of the phytochrome superfamily to shorter wavelengths of visible light. Blue/green light sensing by a well-studied subfamily of CBCRs proceeds via a photolabile thioether linkage to a second cysteine fully conserved in this subfamily. In the present study, we show that dual-cysteine photosensors have repeatedly evolved in cyanobacteria via insertion of a second cysteine at different positions within the bilin-binding GAF domain (cGMP-specific phosphodiesterases, cyanobacterial adenylate cyclases, and formate hydrogen lyase transcription activator FhlA) shared by CBCRs and phytochromes. Such sensors exhibit a diverse range of photocycles, yet all share ground-state absorbance of near-UV to blue light and a common mechanism of light perception: reversible photoisomerization of the bilin 15,16 double bond. Using site-directed mutagenesis, chemical modification and spectroscopy to characterize novel dual-cysteine photosensors from the cyanobacterium *Nostoc punctiforme* ATCC 29133, we establish that this spectral diversity can be tuned by varying the light-dependent stability of the second thioether linkage. We also show that such behavior can be engineered into the conventional phytochrome Cph1 from *Synechocystis* sp. PCC6803. Dual-cysteine photosensors thus allow the phytochrome superfamily in cyanobacteria to sense the full solar spectrum at the earth surface from near infrared to near ultraviolet.

biliprotein | optogenetics | photoreceptor | UV-A sensor

Phytochromes are well-known red/far-red photoreceptors with linear tetrapyrrole (bilin) chromophores that are widely distributed in photosynthetic and nonphotosynthetic organisms (1–3). In seed plants, phytochromes are critical regulators of photomorphogenesis, triggering developmental cascades in response to the availability of photosynthetically useful red light (4). Bacterial phytochromes regulate light harvesting in nonoxygenic photosynthetic bacteria and have been implicated in quorum sensing in *Pseudomonas aeruginosa* (5–7), whereas fungal phytochromes can trigger sexual development in response to red/far-red light (8). The related cyanobacteriochrome photosensors RcaE and CcaS regulate expression of cyanobacterial light-harvesting phycobiliproteins, responding to green and red light in a process known as complementary chromatic acclimation (9–12). Photosensors within the phytochrome superfamily thus transduce photobiological inputs to signaling pathways that regulate a wide range of biological responses.

Phytochromes characteristically photoconvert between stable red-absorbing (P_r) and far-red-absorbing (P_{fr}) forms in a red/far-red photocycle (13). This spectral sensitivity has attracted attention for fluorescent probe development (14, 15) and optogenetics (16–18). Light absorption triggers isomerization of a thioether-linked bilin chromophore buried within a conserved pocket in a specific type of GAF domain (cGMP-specific phosphodiesterases, cyanobacterial adenylate cyclases, and formate hydrogen lyase transcription activator FhlA), a conserved α/β fold found in a wide range of signaling proteins (Fig. 1*A*). In most phytochromes, the GAF domain is found as part of a knotted PAS-GAF-PHY photosensory core module required for full red/far-red reversibility (19–21).

Cyanobacterial photoswitches with phytochrome-related GAF domains have been termed cyanobacteriochromes (CBCRs) (22). CBCRs exhibit more diverse spectral sensitivities and domain architectures than phytochromes, and CBCR GAF domains are sufficient for full reversible photochemistry (22). CBCRs and cyanobacterial phytochromes such as Cph1 (Slr0473) and Cph2 (Sll0821) from *Synechocystis* sp. PCC6803 all share a conserved GAF-domain Cys residue required for phycocyanobilin (PCB) attachment (22, 23). Isolated GAF domains of Cph1 and Cph2 lacking one or more adjacent photosensory domain (s) are insufficient for stable, reversible photoconversion, but individual CBCR GAF domains are typically competent on their own. In this work, we therefore define phytochromes as bilin-based photosensors with PAS-GAF-PHY tridomain modules and CBCRs as those with evolutionarily related, bilin-binding GAF domains (13). The blue/green sensor SyPixJ1 (Sll0041) was the first CBCR to be photochemically characterized (24), and CBCRs with green/red and red/green cycles have been subsequently described (11, 12, 25, 26). CBCRs thus tune the red-absorbing PCB chromophore to detect the entire visible light spectrum, and CBCRs exhibiting similar photocycles appear to group together into subfamilies (Fig. 1*B* and refs. 22 and 27).

The blue/green subfamily of CBCRs has attracted the most attention to date. Acid denaturation of the blue/green CBCR TePixJ (Tll0569) implicates the PCB isomer phycoviolobilin (PVB; Fig. S1) as its chromophore (28), whereas circular dichroism (CD) spectra of the related blue/green CBCR Tlr0924 support a PCB-based chromophore (27). A second Cys conserved in TePixJ and Tlr0924 is essential for blue light absorption and blue/green photochemistry (27, 29, 30). This second Cys is part of a larger Asp-Xaa-Cys-Phe (DXCF) motif unique to the blue/green CBCR subfamily. Recently, TePixJ was shown to isomerize PCB to PVB slowly after initial assembly (30). A photolabile thioether linkage between the second Cys (DXCF Cys) and the C10 position of PVB (Fig. S1) thus explains the blue/green photocycle of the DXCF CBCRs reported to date (30).

Here we present evidence that dual-cysteine bilin photosensors have evolved independently multiple times in cyanobacteria. We have identified a second class of dual-cysteine CBCRs exhibiting broad spectral diversity, with a wavelength range extending from the near-UV (300–400 nm, hereafter abbreviated as UV) to the orange region of the spectrum. We also report the surprising discovery of a dual-cysteine phytochrome encoded by the Cph1-related *NpF1183* locus from the filamentous cyanobacterium

Author contributions: N.C.R. and J.C.L. designed research; N.C.R. and S.S.M. performed research; S.S.M. and K.F. contributed new reagents/analytic tools; N.C.R., S.S.M., and J.C.L. analyzed data; and N.C.R. and J.C.L. wrote the paper.

The authors declare no conflict of interest.

[1]To whom correspondence should be addressed. E-mail: jclagarias@ucdavis.edu.

This article contains supporting information online at www.pnas.org/lookup/suppl/doi:10.1073/pnas.1107844108/-/DCSupplemental.

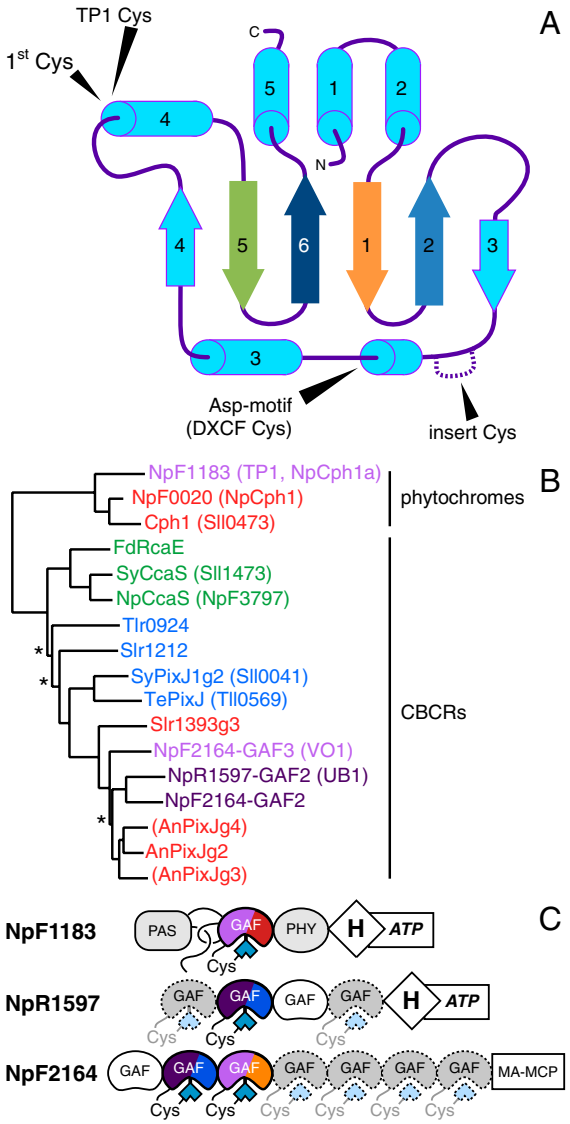

Fig. 1. Evolution of the photosensory GAF domain of phytochromes and CBCRs. (*A*) A topology diagram of the GAF domain, with the conserved "first Cys" and the three types of "second Cys" indicated. The first, second, fifth, and sixth beta strands are color-coded to match the sequence alignment in Fig. S3. (*B*) A neighbor-joining tree is shown for the GAF domains of published CBCRs and proteins described in this study, with names color-coded by ground-state absorbance. Branches with bootstrap values below 67% are indicated with an asterisk. Domains in parentheses bind bilin, but are photochemically inert (25). (*C*) Domain cartoons are shown for the proteins described in this work. CBCRs are color-coded by their photocycles, with near-UV absorbance represented by deep purple. Dashed GAF domains contain the first Cys, but have not yet been described.

Nostoc punctiforme ATCC 29133. This violet-absorbing phytochrome exhibits a unique trichromatic photocycle, and introduction of the equivalent second Cys into *Synechocystis* Cph1 also yields a violet-absorbing phytochrome. These studies suggest that additional photosensory diversity remains yet to be discovered within the phytochrome superfamily.

Results

NpF2164-GAF3 Is a Violet/Orange Dual-Cysteine CBCR. The genome of *N. punctiforme* harbors the largest number of phytochromes and CBCRs reported to date, permitting an extensive survey of CBCR photosensory diversity. The most complex of these potential photosensors is that encoded by the *NpF2164* locus, a protein harboring six CBCR GAF domains (Fig. 1*C*). When compared to previously described CBCRs, the second and third GAF domains of NpF2164 are most closely related to the previously characterized red/green CBCRs AnPixJg2 and Slr1393g3 (Fig. 1*B* and refs. 25 and 26). Surprisingly, recombinant NpF2164-GAF3 coexpressed with a PCB biosynthetic operon in *Escherichia coli* exhibited a violet-absorbing ground state that could be reversibly photoconverted into an orange-absorbing state (Fig. 2*A* and Table S1). In the absence of a described function for *NpF2164*, we therefore give this GAF domain the working name VO1 to denote its violet/orange photocycle. Acid denaturation of VO1 revealed a single bilin population, consistent with a PCB adduct that photoconverts between a *15Z* configuration in the native violet-absorbing state and a *15E* configuration in the native orange-absorbing state (Fig. S2*A* and Table S2). Incorporation of the more conjugated PCB analog phytochromobilin (PΦB) resulted in a large red shift of the native *15Z* ground state (Fig. 2*B*), a smaller red shift of the *15E* state, and small red shifts of both denatured species relative to the PCB adduct (Table S2). Database searches with the VO1 sequence identified a subfamily of approximately 30 proteins containing sequence hallmarks of red/green CBCRs but defined by a large insert relative to such proteins (Fig. S3). This insert contained a conserved cysteine residue (Cys546 in VO1) as part of a weakly conserved Cys-Xaa-Xaa-Arg/Lys (CXXR/K) motif.

To test whether Cys546 was required for the VO1 photocycle, we expressed the C_{546}A mutant protein as an intein-CBD fusion. Purified mutant protein absorbed red rather than violet light, and irradiation with either red or violet light produced no significant changes in the spectrum (Fig. 3*A*). Only trace amounts of orange photoproduct could be observed in difference spectra (Fig. S2*B*). During purification of this mutant protein, we observed color changes both upon addition of dithiothreitol (DTT) for on-column intein cleavage and during subsequent dialysis. DTT treatment of purified C_{546}A protein afforded modest reduction

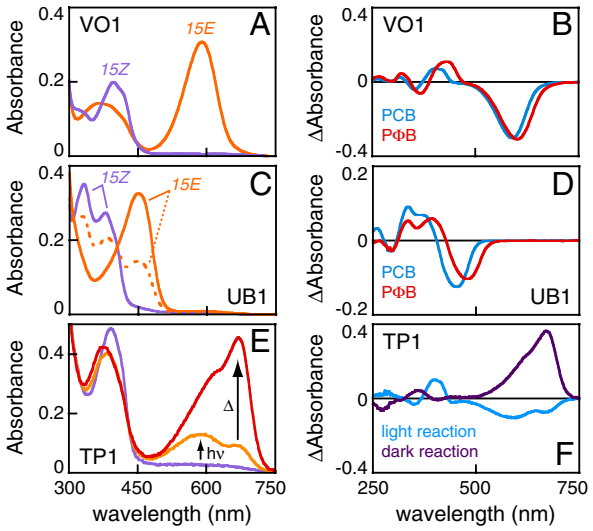

Fig. 2. Three newly identified dual-Cys biliprotein photosensors from *Nostoc punctiforme*. (*A*) Absorbance spectra are shown for VO1 with PCB. (*B*) Photochemical difference spectra are shown for VO1 with PCB (blue) and PΦB (red) chromophores. (*C*) Absorbance spectra are shown for UB1 with PCB. The photoequilibrium spectrum produced by 400 nm illumination is dashed orange, whereas that produced by 334 nm illumination is solid orange. (*D*) Photochemical difference spectra are shown for UB1 with PCB (blue) and PΦB (red) chromophores. (*E*) Absorbance spectra are shown for TP1 in the dark-adapted ground state (purple), after illumination with 400 ± 35 nm light (orange), and after subsequent incubation in darkness at 25 °C for 20 min (red). (*F*) Difference spectra are shown for photoconversion of TP1 with 400 nm light (blue) and for the subsequent thermal evolution of the *15E* photoproduct (deep purple).

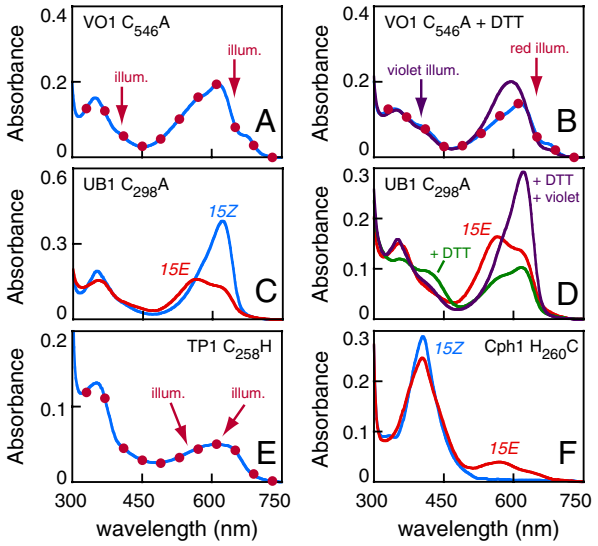

Fig. 3. Identification of novel second Cys residues. (*A*) Absorbance spectra of C_{546}A VO1. Illumination of the ground state (blue trace) with red light (650 ± 20 nm) or violet light (400 ± 35 nm) light produced indistinguishable spectra (red circles). (*B*) C_{546}A VO1 supplemented with 50 mM DTT in the ground state (blue trace) and after illumination with saturating red light (red circles) or violet light (purple trace). (*C*) C_{298}A UB1 in the *15Z* (blue) and *15E* (red) states. (*D*) C_{298}A UB1 is shown in the *15E* state before (red) and after (green) addition of 50 mM DTT. Illumination with violet light after addition of DTT regenerated the *15Z* state (purple). (*E*) Absorbance spectra of C_{258}H TP1. Illumination of the ground state (blue) with 600 ± 20 nm or 550 ± 35 nm light resulted in indistinguishable spectra (red circles). (*F*) Absorbance spectra are shown for H_{260}C Cph1 in the ground state (blue) and after illumination with saturating 400 ± 35 nm light (red).

of absorbance in the red region and slight enhancement of violet absorbance, but DTT did not enhance formation of the photoproduct in response to red illumination (Fig. 3*B* and Fig. S2*B*). However, the combination of DTT and violet illumination led to efficient formation of an orange-absorbing species similar to that produced by violet irradiation of the wild type (Fig. 3*B* and Table S2). By contrast, DTT treatment did not influence wild-type VO1 (Fig. S2*B*). Cys546 is therefore required for the violet/orange photocycle of VO1, and DTT can restore wild-type forward photochemistry to the C_{546}A mutant. VO1 is thus a previously unrecognized violet/orange dual-Cys CBCR.

Insert-Cys CBCRs Are a Spectrally Diverse Subfamily of Dual-Cysteine CBCRs. Two other members of this subfamily of CBCRs were found in the genome of *N. punctiforme*: GAF2 of NpF2164 itself, and GAF2 of NpR1597 (Fig. 1*C* and Fig. S3). The GAF domains of both proteins were expressed as intein-CBD fusions and purified. NpR1597-GAF2 exhibited a UV-absorbing ground state with maxima at 378 and 334 nm (Fig. 2*C*). Irradiation of the longer wavelength transition (400 ± 35 nm) resulted in modest, yet reversible, formation of a photoproduct absorbing blue light (448 nm; Tables S1 and S2); we therefore give this protein the working name UB1 (UV/blue photocycle, protein 1). Incorporation of PΦB into UB1 resulted in large red shifts for both photostates (Fig. 2*D*). NpF2164-GAF2 exhibited a very similar photocycle (Fig. S2), and denaturation analysis revealed the presence of PCB and not PVB in both UB1 and NpF2164-GAF2 (Fig. S2*A* and Table S2).

UB1 exhibited efficient reversibility (Table S1), so it was chosen for further study of this previously unrecognized photocycle. Cys298, the "insert Cys" equivalent to Cys546 of VO1, was mutated to Ala to confirm its importance for the UV-absorbing ground state. As expected, C_{298}A UB1 exhibited a red-absorbing ground state (Fig. 3*C*). Unlike C_{546}A VO1, however, this protein was able to photoconvert to a blue-shifted *15E* photoproduct, somewhat reminiscent of AnPixJ (25). Addition of DTT to either photostate resulted in modest depletion of long-wavelength species and formation of products in the violet to blue region of the spectrum (Fig. S2*E*). Illuminating the *15E* photoproduct with violet light in the presence of DTT efficiently restored the ground state (Fig. 3*D*), and red illumination produced different photoproducts in the presence or absence of DTT (Fig. S2*E*). These data are consistent with formation of a DTT adduct. They also confirm the importance of Cys298 for the UV/blue photocycle of UB1 and define another subfamily of spectrally diverse CBCRs based on the presence of the insert Cys.

Insert-Cys CBCRs Can Function as UV Sensors. Illumination of UB1 with violet light (400 ± 5 nm) resulted in incomplete photoconversion, apparently due to spectral overlap between the first transition and the photoproduct (Table S1). By contrast, illumination of the shorter wavelength transition (334 ± 5 nm) afforded higher yields of the same photoproduct (Fig. 2*C* and Fig. S2*F*) at much lower rates (Fig. S2*G*). Slow photoproduct formation was even observed with 280 nm illumination, albeit with an intermediate yield at photoequilibrium (Fig. S2 *F* and *G*). We therefore examined the effect of 334 and 280 nm illumination on the violet/orange sensor, VO1. Formation of apparently normal photoproduct was observed at both wavelengths, again at much lower rates than seen with violet excitation (Fig. S2*H*). The PΦB adduct of VO1 also behaved similarly. These results underscore the broad spectral sensitivity of the CBCR family: For different CBCRs, photoconversion can be supported by light from the red region of the spectrum all the way down to the absorption of the aromatic amino acids in the CBCR protein scaffold.

Natural and Designed Dual-Cysteine Phytochromes. The *NpF0020* and *NpF1183* loci of *N. punctiforme* encode knotted phytochromes closely related to Cph1 (Fig. 1*A*). To our surprise, the recombinant PAS-GAF-PHY module from *NpF1183* (NpCph1a in ref. 2) was not a red/far-red photosensor. Instead, this protein exhibited ground-state absorbance at the violet edge of the visible spectrum (Fig. 2*E*, violet trace). Violet illumination resulted in formation of an orange-absorbing photoproduct that thermally converted to a red-absorbing species (Fig. 2 *E* and *F*). We therefore give this protein the working name TP1 (trichromatic phytochrome 1). The red-absorbing species formed thermally by TP1 after illumination was similar to red-absorbing *15E* states described for the green/red CBCRs SyCcaS and NpCcaS (11, 12). Whereas low expression of TP1 hindered detailed analysis, acid denaturation of the red-absorbing state confirmed the presence of *15E* PCB (Fig. S2*A* and Table S2). Similar to VO1 and UB1, TP1 could be efficiently cycled back to its violet-absorbing ground state (Table S1).

In TP1, the conserved His260 of Cph1 is replaced with a Cys (Cys258). The C_{258}H mutant of TP1 absorbed red light (Fig. 3*E*), although chromophore incorporation and photoconversion were severely compromised (Table S1). Strikingly, introducing the converse H_{260}C mutant into Cph1 resulted in violet absorbance (Fig. 3*F*). H_{260}C Cph1 was able to form a modest amount of an orange-absorbing photoproduct, albeit with poor reversibility (Table S1). No thermal conversion of this photoproduct to a red-absorbing form was observed for H_{260}C Cph1, demonstrating that other mutations are required to confer the trichromatic photocycle of TP1 upon red/far-red phytochromes. These data demonstrate that TP1 is a dual-Cys phytochrome and identify its second Cys as both necessary and sufficient for violet absorbance within a cyanobacterial phytochrome scaffold.

Spectral Tuning and Dual-Cys Photocycles. VO1 and UB1 provide a case study in spectral tuning by dual-Cys photosensors. We first examined both photocycles by CD spectroscopy. The *15Z* states

of both proteins exhibited negative CD for the long-wavelength band with either PCB or PΦB, as did the orange-absorbing *15E* photoproduct of VO1 (Fig. S4). The blue-absorbing *15E* photoproduct of UB1 instead exhibited weak positive CD, implicating a stereochemically distinct photocycle (31). A similar inversion of CD was also observed in the UV/blue photocycle of NpF2164-GAF2 (Fig. S2*D*).

We next compared PCB and PΦB adducts, which only differ in the C18 side chain (Fig. S1). C10 adducts generate two conjugated π systems associated with the A/B- and C/D-ring systems (Fig. S1). Substitution of PΦB for PCB would thus influence the absorption associated with the C/D-ring system, but not the transition associated with the A/B-ring system. Detailed comparison of PCB and PΦB adducts for VO1 and UB1 revealed such a pattern (Fig. S4): The lowest energy transition of the *15Z* state has a large red shift of 16–20 nm for the PΦB adduct, but the second transition has almost none (0–2 nm). We were unable to resolve the second transition in *15E* UB1 unambiguously, but the long-wavelength transition displayed a significant red shift in the PΦB adduct, as did both transitions for *15E* VO1.

The red-shift pattern observed for VO1 is consistent with a labile second linkage in this protein: both absorption transitions are red-shifted for the *15E* state, indicating a single conjugated system in this state. With such a photolabile linkage, we expected that the second Cys thiol would be accessible to the thiol-specific reagent iodoacetamide (IAM) in the *15E* state but blocked in the *15Z* state. We therefore examined the effect of IAM on reverse photoconversion (*15E*-to-*15Z*) for both UB1 and VO1 (Fig. 4*A*, *Upper*). IAM treatment minimally affected the *15E* spectra, and the normal *15Z* state of UB1 could be readily regenerated. By contrast, orange illumination of the IAM-treated *15E* state of VO1 yielded a substantial amount of a red-absorbing species similar to that observed for the C_{546}A mutant protein. IAM-treated *15Z* states of both UB1 and VO1 retained the ability to photocycle to their *15E* states and back again without substantial accumulation of trapped species (Fig. 4*B*, *Upper*). Only the orange-absorbing *15E* form of VO1 was sensitive to IAM treatment; therefore, a Cys residue in *15E* VO1 is accessible to IAM and essential for regeneration of the violet-absorbing ground state.

We next tested the sensitivity of UB1 and VO1 to hydrogen peroxide. Both photostates of UB1 were rapidly converted to red-shifted species by peroxide (Fig. 4 *A* and *B*, *Lower Left*), demonstrating that UB1 resistance to IAM is not due to general steric occlusion from small-molecule reagents. Peroxide treatment of the violet-absorbing *15Z* ground state of VO1 also yielded a red-absorbing species (Fig. 4*B*, *Lower Right*). By contrast, the *15E* state of VO1 was only slightly affected by peroxide, yet illumination yielded a red-absorbing species rather than regenerating the ground state (Fig. 4*A*, *Lower Right*). Control experiments confirmed that photochemistry of denatured *15E* samples was not affected by the presence of peroxide on this timescale (Fig. S5). The absorption maximum of native Y_{176}H Cph1, which absorbs red light, was not shifted by peroxide treatment, but the violet-absorbing H_{260}C mutant was converted to a species absorbing at longer wavelengths (Fig. S5). Taken together, these data indicate that the second thioether linkage at C10 is sensitive to peroxide-induced cleavage but refractory to modification by IAM. We therefore conclude that the spectral sensitivity of the *15E* photoproduct of these two proteins is tuned by the stability of the second linkage to C10: the second linkage is stable in UB1, but photolabile in VO1.

Discussion

We report the discovery of two additional types of GAF-based bilin photosensors with ground-state absorption in the UV to violet spectral region. Both types require two GAF domain cysteine residues. Unlike DXCF CBCRs such as TePixJ and Tlr0924 (27, 28, 30), the insert-Cys CBCRs do not isomerize the PCB

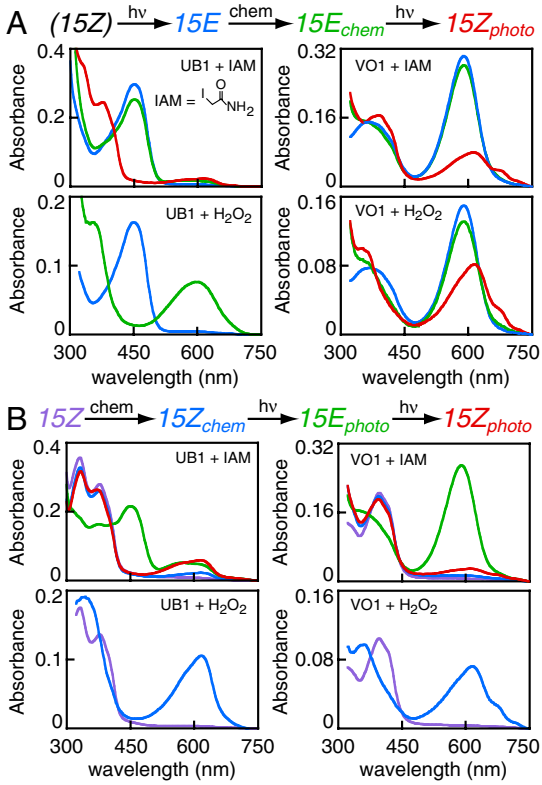

Fig. 4. Characterization of the second linkage in VO1 and UB1. (*A*) Reverse photoconversion (*15E* to *15Z*) was examined after treatment with IAM or H_2O_2. Photoproteins were converted to the *15E* state (blue), followed by reaction with IAM or H_2O_2 in darkness to yield *15E* chemical products (green). The *15E* chemical products were then illuminated when appropriate to generate *15Z* photoproducts (red). Blue traces for H_2O_2 treatment are scaled to reflect the 1:1 dilution of sample upon peroxide addition. (*B*) Forward photoconversion was similarly examined. The *15Z* photoproteins (purple) were treated with IAM or H_2O_2 in darkness to yield *15Z* chemical products (blue), which were then cycled to the *15E* state (green) and back (red).

precursor to PVB. Nevertheless, denaturation analysis demonstrates that all known classes of dual-cysteine photosensor share a common primary photochemical event: photoisomerization of the 15/16 double bond (Table S2 and refs. 28 and 30). These results also show that the CBCR family effectively provides complete coverage of the spectral region between the red/far-red photocycles of phytochromes and the protein absorbance band at 280 nm (Fig. 5*A*), underscoring the flexibility of this family of photoswitches.

The insert-Cys CBCRs, possessing a second cysteine within an insert (Fig. 1*A* and Fig. S3), are the most widely distributed of these previously undescribed sensors. Members of this subclass are most related to the red/green CBCRs AnPixJ and Slr1393g3 (Fig. 1*B* and Fig. S3), so they are likely to have arisen independently of the DXCF dual-cysteine CBCR family. Database searches identify members of this subfamily in many cyanobacteria, including both marine and freshwater species and both unicellular and filamentous forms (Table S3). By contrast, the violet-sensing phytochrome TP1 appears unique to date. It is therefore clear that dual-cysteine biliprotein photosensors have evolved independently at least three times in cyanobacteria for sensing light in the UV-to-blue spectral region.

We propose that the role of the second cysteine in dual-Cys photocycles is conserved. Mutagenesis of the second cysteine results in a red-absorbing mutant protein in Tlr0924 (27), TePixJ (29, 30), VO1, UB1, and TP1. In all cases except UB1, mutation of the second Cys also compromises photochemistry, indicating

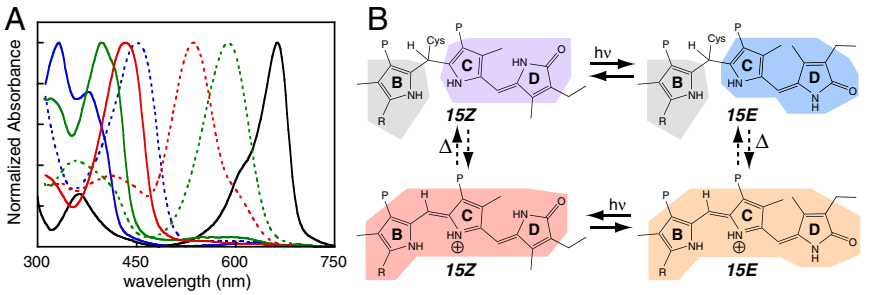

Fig. 5. Dual-cysteine photosensors. (*A*) Spectral coverage of representative dual-Cys photosensors. Absorbance spectra are shown for UB1 (blue), VO1 (green), and Tlr0924 [red (27)] in the *15Z* (solid) and *15E* (dashed) states. Wild-type *15Z* Cph1 is shown in black for comparison. (*B*) A general dual-Cys photocycle. In the dark-adapted *15Z* ground state (*Upper Left*), there is a covalent linkage between C10 and the second Cys. Light induces 15/16 photoisomerization to produce a *15E* species with an intact second linkage (*Upper Right*). In UB1, this species is stable. In VO1, the second linkage is labile in the *15E* state, red-shifting the photoproduct absorbance (*Lower Right*). Photoconversion produces a red-shifted species (bottom left). Only the B-, C-, and D-rings are shown; isomerization of the A-ring allows further spectral tuning.

that the second cysteine typically facilitates *15Z*-to-*15E* photoisomerization of these proteins. This is consistent with the photochemical rescue of C_{546}A VO1 by the thiol reagent DTT (Fig. 3) and the observed *15Z*-to-*15E* photoconversion of isolated bilins with blue light in the presence of 2-mercaptoethanol (32). A thioether linkage between the second cysteine in dual-cysteine photosensors and the C10 position of the *15Z* bilin chromophore is also consonant with the known reactivity of bilins toward nucleophilic reagents (33–35) and the spectra of phycocyanorubin and phytochromorubin (36). Chemical modification experiments support the following conclusions: one, that the second linkage in VO1 is broken following photoconversion to the orange-absorbing *15E* state, whereupon Cys546 becomes accessible to IAM modification; and, two, that the second linkage in UB1 is stable in both UV- and blue-absorbing states. Intriguingly, the CD spectra of VO1 and UB1 indicate that stable and labile linkages can be associated with stereochemically distinct photoproducts.

Based on these observations, we propose a consensus dual-cysteine photocycle that rationalizes the observed blue/green, UV/blue, violet/orange and violet/red cases (Fig. 5*B*). All species share a covalent linkage between the conserved GAF-domain first Cys and the A-ring ethylidene group of PCB or PVB (Fig. S1). In the *15Z* ground state, a second linkage is present between the chromophore C10 atom and a second Cys unique to each of the three classes. The primary photoreaction for all dual-cysteine photosensors yields a *15E* species that initially retains the second linkage. For UB1 and NpF2164-GAF2, the second linkage remains stable in the *15E* state. In the other proteins, the second linkage is broken thermally after photoisomerization, resulting in a species with absorbance at longer wavelengths. If the protein is able to convert PCB adducts into PVB adducts (30), this *15E* species will have green absorbance. If the bilin remains a PCB adduct, this species will absorb in the orange to red region. With labile linkage dual-cysteine photosensors, photoisomerization of the *15E* state yields a long-wavelength *15Z* intermediate that ultimately regenerates the ground state via restoration of the second linkage.

The present work also holds interesting implications for photobiology, photoprotein engineering, and synthetic biology (15, 16, 37). Dual-cysteine CBCRs are modular photosensors well suited to spectral tuning of an engineered response, for instance to allow variation in tissue penetrance or to avoid intrinsic photobiological effects. Chemical rescue of second Cys mutants in the insert-Cys subfamily by DTT raises the possibility of natural or engineered cryptic photosensors, which are only photoactive in the presence of physiologically relevant thiols such as glutathione or in the presence of another protein that supplies a Cys residue. Moreover, the surprising ease with which the red/far-red phytochrome Cph1 can be converted into a dual-Cys phytochrome raises the possibility that equivalent mutations could have similar effects in the phytochromes of higher plants. Finally, the repeated evolution of dual-Cys sensors in cyanobacteria makes it plausible that analogous high-energy photosensory biliproteins might be present in any organism able to synthesize or scavenge linear tetrapyrroles. Such proteins could lack the first Cys, or might not even use a recognizable GAF fold, yet would still use a thioether at C10 to allow tetrapyrroles to sense blue and UV light. Ubiquitous photosensitizing pigments such as flavins demonstrate the need for such systems, even in nonphotosynthetic organisms (38).

Materials & Methods

Computational Techniques. To identify CBCRs with the insert-Cys found in VO1, BLAST (39) searches used either VO1 or UB1 as query sequences. The resulting CBCRs were aligned with MUSCLE (40) followed by manual addition of AnPixJg2, *Synechocystis* Cph1, and TePixJ. Phylogenetic trees were constructed using the neighbor-joining algorithm of CLUSTALW (41). Unique residues in TP1 were identified using a published phytochrome sequence alignment (2) and a developmental version of HOMOLMAPPER (42).

Protein Expression and Purification. Appropriate primers were used to amplify regions of interest from *N. punctiforme* genomic DNA [generous gift of Elsie L. Campbell and Jack Meeks, University of California (UC), Davis]. Specific protein regions cloned for expression are reported in Fig. S6. PCR products were digested with *Nco*I and *Sma*I and cloned into pBAD-Cph1-CBD (31). C-terminal intein-CBD fusion proteins were coexpressed with pPL-PCB, encoding biosynthetic machinery for PCB production in *E. coli* strain LMG194 (43). Coproduction of PΦB used a published modification of this system (37). Purification using chitin resin (NEB) followed a previously described procedure (31), with final dialysis against TKKG buffer (25 mM TES-KOH pH 7.8, 100 mM KCl, 10% (v/v) glycerol). For production of C-terminally His_6-tagged VO1, we cloned the equivalent region into pET28a-RcaE (generous gift of Yuu Hirose, University of Tokyo, Tokyo) using *Nco*I and *Bam*HI sites to keep the C-terminal His_6 tag and associated sequences in-frame. Expression then used *E. coli* strain C41[DE3] (44) with plasmid pKT271 (generous gift of Takayuki Kohchi, Kyoto University, Kyoto) for PCB synthesis as described (45), and protein was purified on Talon resin (Clontech) using an imidazole gradient (30–430 mM) with subsequent dialysis into TKKG. Approximately 5 μg protein was analyzed by SDS-PAGE using standard procedures and apparatus (BioRad) followed by semidry transfer to PVDF membranes, staining with amido black for visualizing total protein, and final zinc blotting to confirm the presence of covalently bound bilin (Fig. S6).

Spectroscopy. Absorbance spectra were acquired at 25 °C on a Cary 50 spectrophotometer modified for illumination from above with a 75 W xenon source and bandpass filters as described (31). Bandpass filters used for triggering photochemistry were 650 nm center/40 nm width, 550 nm/70 nm, 600 nm/40 nm, 500 nm/25 nm, 450 nm/25 nm, 400 nm/70 nm, 334 nm/10 nm, and 280 nm/10 nm. Denaturation assays used either guanidinium chloride/1% HCl (46) or 1:6 dilution with 6 M guanidinium chloride/100 mM citric acid, pH 2.2. No difference was observed between these two conditions. Treatment with 3 mM IAM was carried out for 20 min at RT in the dark using freshly prepared stock solutions. IAM concen-

tration was experimentally confirmed using a published extinction coefficient (47). Treatment with H_2O_2 was performed by addition of an equal volume of commercial 30% H_2O_2 for 2 min, followed immediately by spectroscopy. DTT was added to indicated concentrations from a freshly prepared 1 M stock. CD spectra were acquired on an Applied Photophysics Chirascan using a 2 nm bandwidth and are reported as baseline-corrected, unsmoothed single scans. Photochemical difference spectra are reported as (*15Z–15E*), whereas the thermal difference spectrum shown for dark evolution of TP1 in Fig. 2*F* is reported as (end-start).

ACKNOWLEDGMENTS. We thank Dr. Yuu Hirose (University of Tokyo) for plasmid pET28a-RcaE and for helpful discussions. We also thank Elsie L. Campbell and Professor Jack Meeks (UC Davis) for the generous gift of *N. punctiforme* genomic DNA, Prof. Takayuki Kohchi (Kyoto University) for the gift of plasmid pKT271, and Professor Kai-Hong Zhao (Huazhong Agricultural University) for α-PEC spectra used as references in Table S2. This work was supported by National Institutes of Health Grant GM068552 (J.C.L) and from Chemical Sciences, Geosciences, and Biosciences Division, Office of Basic Energy Sciences, Office of Science, US Department of Energy DOE DE-FG02-09ER16117 (J.C.L.).

1. Montgomery BL, Lagarias JC (2002) Phytochrome ancestry. Sensors of bilins and light. *Trends Plant Sci* 7:357–366.
2. Rockwell NC, Su YS, Lagarias JC (2006) Phytochrome structure and signaling mechanisms. *Annu Rev Plant Biol* 57:837–858.
3. Auldridge ME, Forest KT (2011) Bacterial phytochromes: More than meets the light. *Crit Rev Biochem Mol Biol* 46:67–88.
4. Franklin KA, Quail PH (2010) Phytochrome functions in Arabidopsis development. *J Exp Bot* 61:11–24.
5. Giraud E, et al. (2002) Bacteriophytochrome controls photosystem synthesis in anoxygenic bacteria. *Nature* 417:202–205.
6. Giraud E, et al. (2005) A new type of bacteriophytochrome acts in tandem with a classical bacteriophytochrome to control the antennae synthesis in *Rhodopseudomonas palustris*. *J Biol Chem* 280:32389–32397.
7. Barkovits K, Schubert B, Heine S, Scheer M, Frankenberg-Dinkel N (2011) Function of the bacteriophytochrome BphP in the RpoS/Las-quorum sensing network of *Pseudomonas aeruginosa*. *Microbiology*.
8. Blumenstein A, et al. (2005) The *Aspergillus nidulans* phytochrome FphA represses sexual development in red light. *Curr Biol* 15:1833–1838.
9. Kehoe DM, Grossman AR (1996) Similarity of a chromatic adaptation sensor to phytochrome and ethylene receptors. *Science* 273:1409–1412.
10. Kehoe DM, Gutu A (2006) Responding to color: The regulation of complementary chromatic adaptation. *Annu Rev Plant Biol* 57:127–150.
11. Hirose Y, Shimada T, Narikawa R, Katayama M, Ikeuchi M (2008) Cyanobacteriochrome CcaS is the green light receptor that induces the expression of phycobilisome linker protein. *Proc Natl Acad Sci USA* 105:9528–9533.
12. Hirose Y, Narikawa R, Katayama M, Ikeuchi M (2010) Cyanobacteriochrome CcaS regulates phycoerythrin accumulation in *Nostoc punctiforme*, a group II chromatic adapter. *Proc Natl Acad Sci USA* 107:8854–8859.
13. Rockwell NC, Lagarias JC (2010) A brief history of phytochromes. *ChemPhysChem* 11:1172–1180.
14. Fischer AJ, Lagarias JC (2004) Harnessing phytochrome's glowing potential. *Proc Natl Acad Sci USA* 101:17334–17339.
15. Shu X, et al. (2009) Mammalian expression of infrared fluorescent proteins engineered from a bacterial phytochrome. *Science* 324:804–807.
16. Levskaya A, Weiner OD, Lim WA, Voigt CA (2009) Spatiotemporal control of cell signalling using a light-switchable protein interaction. *Nature* 461:997–1001.
17. Möglich A, Moffat K (2010) Engineered photoreceptors as novel optogenetic tools. *Photochem Photobiol Sci* 9:1286–1300.
18. Tabor JJ, Levskaya A, Voigt CA (2011) Multichromatic control of gene expression in *Escherichia coli*. *J Mol Biol* 405:315–324.
19. Wagner JR, Brunzelle JS, Forest KT, Vierstra RD (2005) A light-sensing knot revealed by the structure of the chromophore binding domain of phytochrome. *Nature* 438:325–331.
20. Essen LO, Mailliet J, Hughes J (2008) The structure of a complete phytochrome sensory module in the Pr ground state. *Proc Natl Acad Sci USA* 105:14709–14714.
21. Yang X, Kuk J, Moffat K (2008) Crystal structure of *Pseudomonas aeruginosa* bacteriophytochrome: photoconversion and signal transduction. *Proc Natl Acad Sci USA* 105:14715–14720.
22. Ikeuchi M, Ishizuka T (2008) Cyanobacteriochromes: A new superfamily of tetrapyrrole-binding photoreceptors in cyanobacteria. *Photochem Photobiol Sci* 7:1159–1167.
23. Wu SH, Lagarias JC (2000) Defining the bilin lyase domain: Lessons from the extended phytochrome superfamily. *Biochemistry* 39:13487–13495.
24. Yoshihara S, Katayama M, Geng X, Ikeuchi M (2004) Cyanobacterial phytochrome-like PixJ1 holoprotein shows novel reversible photoconversion between blue- and green-absorbing forms. *Plant Cell Physiol* 45:1729–1737.
25. Narikawa R, Fukushima Y, Ishizuka T, Itoh S, Ikeuchi M (2008) A novel photoactive GAF domain of cyanobacteriochrome AnPixJ that shows reversible green/red photoconversion. *J Mol Biol* 380:844–855.
26. Zhang J, et al. (2010) Fused-gene approach to photoswitchable and fluorescent biliproteins. *Angew Chem Intl Ed Engl* 49:5456–5458.
27. Rockwell NC, et al. (2008) A second conserved GAF domain cysteine is required for the blue/green photoreversibility of cyanobacteriochrome Tlr0924 from *Thermosynechococcus elongatus*. *Biochemistry* 47:7304–7316.
28. Ishizuka T, Narikawa R, Kohchi T, Katayama M, Ikeuchi M (2007) Cyanobacteriochrome TePixJ of *Thermosynechococcus elongatus* harbors phycoviolobilin as a chromophore. *Plant Cell Physiol* 48:1385–1390.
29. Ulijasz AT, et al. (2009) Cyanochromes are blue/green light photoreversible photoreceptors defined by a stable double cysteine linkage to a phycoviolobilin-type chromophore. *J Biol Chem* 284:29757–29772.
30. Ishizuka T, et al. (2011) The cyanobacteriochrome, TePixJ, isomerizes its own chromophore by converting phycocyanobilin to phycoviolobilin. *Biochemistry* 50:953–961.
31. Rockwell NC, Shang L, Martin SS, Lagarias JC (2009) Distinct classes of red/far-red photochemistry within the phytochrome superfamily. *Proc Natl Acad Sci USA* 106:6123–6127.
32. Falk H (1989) *The Chemistry of Linear Oligopyrroles and Bile Pigments* (Springer, Vienna) p 621.
33. Kufer W, Scheer H (1982) Rubins and Rubinoid Addition Products from Phycocyanin. *Z Naturforsch* 37c:179–192.
34. Chen LY, Kinoshita H, Inomata K (2009) Synthesis of doubly locked 5Zs15Za-biliverdin derivatives and their unique spectral behavior. *Chem Lett* 38:602–603.
35. Tu JM, et al. (2009) Toward a mechanism for biliprotein lyases: revisiting nucleophilic addition to phycocyanobilin. *J Am Chem Soc* 131:5399–5401.
36. Terry MJ, Maines MD, Lagarias JC (1993) Inactivation of phytochrome- and phycobiliprotein-chromophore precursors by rat liver biliverdin reductase. *J Biol Chem* 268:26099–26106.
37. Fischer AJ, et al. (2005) Multiple roles of a conserved GAF domain tyrosine residue in cyanobacterial and plant phytochromes. *Biochemistry* 44:15203–15215.
38. van der Horst MA, Key J, Hellingwerf KJ (2007) Photosensing in chemotrophic, non-phototrophic bacteria: let there be light sensing too. *Trends Microbiol* 15:554–562.
39. Altschul SF, et al. (1997) Gapped BLAST and PSI-BLAST: a new generation of protein database search programs. *Nucleic Acids Res* 25:3389–3402.
40. Edgar RC (2004) MUSCLE: Multiple sequence alignment with high accuracy and high throughput. *Nucleic Acids Res* 32:1792–1797.
41. Higgins DG, Thompson JD, Gibson TJ (1996) Using CLUSTAL for multiple sequence alignments. *Methods Enzymol* 266:383–402.
42. Rockwell NC, Lagarias JC (2007) Flexible mapping of homology onto structure with homolmapper. *BMC Bioinformatics* 8:123.
43. Gambetta GA, Lagarias JC (2001) Genetic engineering of phytochrome biosynthesis in bacteria. *Proc Natl Acad Sci USA* 98:10566–10571.
44. Miroux B, Walker JE (1996) Over-production of proteins in *Escherichia coli*: Mutant hosts that allow synthesis of some membrane proteins and globular proteins at high levels. *J Mol Biol* 260:289–298.
45. Mukougawa K, Kanamoto H, Kobayashi T, Yokota A, Kohchi T (2006) Metabolic engineering to produce phytochromes with phytochromobilin, phycocyanobilin, or phycoerythrobilin chromophore in *Escherichia coli*. *FEBS Lett* 580:1333–1338.
46. Shang L, Rockwell NC, Martin SS, Lagarias JC (2010) Biliverdin amides reveal roles for propionate side chains in bilin reductase recognition and in holophytochrome assembly and photoconversion. *Biochemistry* 49:6070–6082.
47. Yuan ZY, Hammes GG (1985) Elementary steps in the reaction mechanism of chicken liver fatty acid synthase. Acylation of specific binding sites. *J Biol Chem* 260:13532–13538.